Advanced Triangle Split Ring Resonator Designs for Enhanced Negative Refractive Index in GHz Frequency Range

Samira A. Mahdi [1]
Thill A.K. Al-musawi [2]
Sundus Y.H. AL-Asadi [3]

[1] Department of Physics, College of Science, Babylon University, Hilla, IRAQ
[2] Department of Physics, College of Science, Al Muthanna University, Samawa, IRAQ
[3] Department of Physics, College of Education for Girls, Kufa University, Kufa, Al-Najaf Province, IRAQ

This work evaluates the characteristics of artificial metamaterials by designing 3D lattice vectors using CST (Computer Simulation Technology). Split ring resonators (SRRs) are modeled as series-resonant LC circuits, with total capacitance represented as a sum of gap capacitance and surface capacitance. These virtual SRRs are created using the dielectric constant of the substrate and the medium in the split- gap. A group of simulations were performed to obtain S-parameters, and the magnetic resonance frequencies of new SRR designs were analyzed. The study provides new constructs of SRRs: (tr-tr) SRR- equilateral concentric triangles, (tr-c) SRR– triangle with circular center and (tr-sq) SRR- triangle with square center. These SRR designs attempt to overcome some of the drawbacks experienced in the conventional SRS, such as scaling difficulties and low performance.

***Keywords*:** Effective permeability; Effective permittivity; Refractive index; SRRRs
Received: 10 December 2024; **Revised:** 12 February; **Accepted:** 19 February 2025

1. Introduction

Left-handed materials (LH materials), or metamaterials with a negative refractive index, indeed exhibit fascinating optical behaviors that differ significantly from conventional materials. These materials adhere to the laws of physics while introducing unique phenomena, such as reversing the direction of refracted light propagation compared to traditional right-handed materials. It's noteworthy that the frequency of light remains unchanged during refraction in LH materials, aligning with fundamental optical principles [1-4]. The metamaterials with negative permeability μ and permittivity ϵ have attracted a range of terminologies to describe their unique properties. Left-handed media refers to the reversed direction of wave propagation and it is highlighted their ability to refract light negatively [5-7]. The permeability (μ) and permittivity (ε) are fundamental to understanding how electromagnetic waves travel through various media. By carefully designing and fabricating materials with tailored μ and ε values, we can create metamaterials that exhibit extraordinary properties not found in nature [8]. In order to provide a magnetic response to applied electromagnetic fields, Pendry et al. [9-12] presented a number of configurations of conducting scattering elements. The SRRs were one of the suggested layouts because they exhibit a particular magnetic resonance at a certain frequency [13]. Such structures have demonstrated that SRR media, when paired with thin rod media, may exhibit left-handed features [14], which can supply negative μ around its resonance frequency and negative permittivity ε [10-13]. Pendry proposed a scheme in which predicted that a pair of concentric SRR would exist. With a current circulating in the rings and a dipolar magnetic field model, an individual SRR functions as a magnetic dipole [15]. The SRR is a pair of parallel and related concentric annular rings with splits in them at their obverse ends [16]. The rings have a tiny space between them and are constructed of a nonmagnetic metal like silver [17]. Splits can be used to create resonance in the SRR unit at wavelengths greater than the diameter of the rings [18]. Negative refractive index metamaterials achieve this unique property by combining subwavelength structures (often smaller than the wavelength of light) in a periodic arrangement [8,19]. These structures interact with electromagnetic waves in a way that effectively reverses the refractive index [20-22]. A wave propagates through a SRR structures, the magnetic response is create by the magnetic field of the wave induces current in the rings [23-26]. The material consists of three-dimensional unit cells of split ring resonators SRR with rods on other side of SRR at X-band microwave frequencies. These tiny structures SRRs resembling split rings, are commonly used in negative refractive index metamaterials [27].

In this paper we studied the electric and the magnetic resonances response of three shapes of SRRs for different orientations of the SRRs with respect to the external electric field (E) and the direction of propagation (k). The effective electric permittivity ε as

well as the magnetic permeability μ will be extracted by the retrieval procedure.

2. Experimental Part

2.1 Comparison among the Artificial Designs

In the engineered materials design, there is the so called bulk metamaterials. They are discrete media made of a combination of unit cells of small electrical size at the frequency of interest [1,6]. A standard procedure was established to design bulk metamaterials with negative parameters at microwave frequencies. This procedure is based on the use of system of SRRs to obtain negative magnetic permeability and an additional metallic wires and plates to obtain negative dielectric permittivity. Thus, the combination of SRRs and metallic wires/plates plays a crucial role in achieving negative magnetic permeability and negative dielectric permittivity at microwave frequencies [4,7,8]. In the current work, we shall theoretically investigate the behavior of resonances (both magnetic and electrical). For a variety of various resonator structures, we first report the measurements and simulations on the single unit cells of SRRs.

The goal is to simultaneously create negative effective permittivity and negative effective permeability in a specific frequency band. Then, we will investigate how different resonator designs and the geometric characteristics of SRRs affect the magnetic resonance frequency. The first step for the construction of a SRR. A metal with no magnetic properties is used to create a ring. When a magnetic field H induces a current, it results in a weak magnetic response. To introduce resonance, a cut is made in the ring. To introduce a resonance, a cut is made in the ring. This step-by-step methodology ensures a systematic approach to exploring and understanding the behavior of SRRs.

The use of SRRs to achieve negative magnetic permeability and the addition of metallic wires to attain negative dielectric permittivity are indeed pioneering in the field of metamaterials. To improve the resonance response, by adding a concentric ring within the first ring, we are optimizing the resonance response. This, combined with the use of rods for negative electric permittivity (ε) and SRR structures for negative magnetic permeability (μ), forms a comprehensive setup to achieve a negative refractive index (n), separated by a distance (d). Consequently, it became possible to develop a new material with the desired electromagnetic responses be obtained, such as negative refractive index. In this paper, the rod was used to get the negative electric permittivity, while the structures SRR were used to get the negative magnetic permeability, thus, the whole structure SRR-rod was formed from the rod and the structure SRR which was used to get the negative refractive index [17,26]. Different structures of the SRR-rod were presented, and the effect of these structures on resonant frequencies and other effective optical parameters like the ε, μ and n are discussed using a simulated S- parameters [13,28]. With the advent of the split ring resonator [1], and its unique electromagnetic properties, much work has been done utilizing these structures as band stop or pass elements. These elements have unique resonances depending on their overall shape and material from which they are constructed [29-34].

Examples of "tr-tr" SRR, "tr-sq" SRR and "tr-c" SRR are shown in figures (1), (2), and (3). Elements fabricated from metal and placed upon a substrate have the ability to manipulate the transmission by acting as band stops through absorption [35]. By etching these elements into a conductive metal sheet with a backing dielectric substrate, a band pass device can be obtained. Not only can these structures be made into useful filters and stops but by manipulating the phase of the incoming radiation, an array of these structures has the ability to act as a flat lens [36]. The split width g= 0.2 mm, metal width wt= 0.2 mm and rod width s= 1.14 mm are detailed for each design. The impact of frequency on S11 and S21 parameters is studied over a broadband range of 10-45 GHz to determine effective frequency ranges. A simulation was done with normal incidence and the magnetic field is polarized with y-axis while the electric field is polarized at x- axis to get S-parameters, with unit cell l= 3 mm, and the effective thickness of material sample is 2.5 μm [35-38]. The values of real parameter S11 of the design of tr-tr starts at 10 GHz increasing to a maximum level at 17.611 GHz, while the peak value of real S21 spectrum was 17.611 GHz, as shown in Fig. (4).

The real values of parameter S11 of the design of sq-tr starts at 10 GHz increasing to the highest possible level at 11.321 GHz, while the peak value of real S21 spectrum was 11.321 GHz also, as in Fig. (5). The values of real parameter S11 of the design of c-tr starts at 10 GHz increasing to the highest possible level at 10.301 GHz, while the peak value of real S21 spectrum was 10.25 GHz, as in Fig. (6). The work region must be approximately between 10 and 24 GHz, as indicated in figures (4-6), as the peaks and band gaps have taken into account the frequency of the SRR resonator, and the values of resonant frequency for the designs tr-tr, sq-tr and c- tr, as shown in table (1).

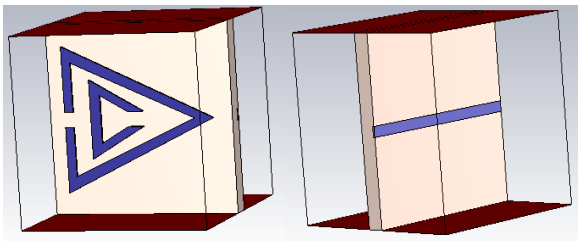

Fig. (1) Typical unit cell of the left-handed structure contains SRR with a metallic rod placed on the dielectric board for triangle-triangle SRR (tr- tr design)

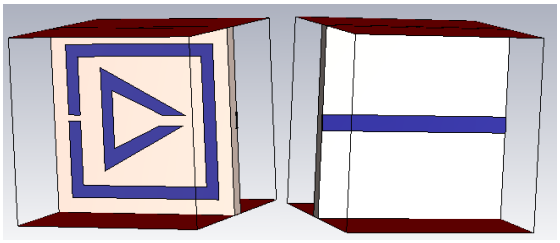

Fig. (2) Typical unit cell of the left-handed structure contains SRR with a metallic rod placed on the dielectric board for square-triangle SRR (sq-tr design)

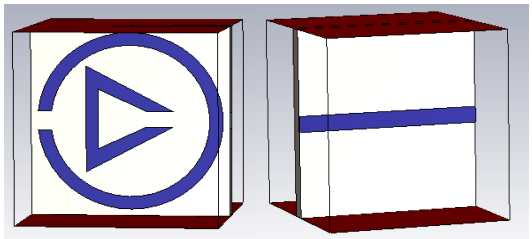

Fig. (3) Typical unit cell of the left-handed structure contains SRR with a metallic rod placed on the dielectric board for circle-triangle SRR (c-tr design)

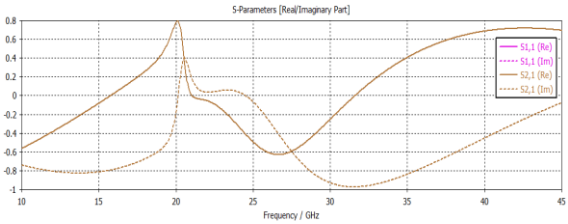

Fig. (4) Real and imaginary elements of the S11 and S21 SRR design parameters for tr-tr design frequency range of 10-45 GHz

2.2 Variation of Geometric Parameters

In this section will discuss the effects of geometrical properties on the properties of the designed material. Effect of split width, effect of gap distances between the rings, thickness of substrate and effect of metal width. Where the split width changed from 0.3 to 0.1 mm, gap distances between the rings changed from 0.3 to 0.1 mm, thickness of substrate changed from 3 to 2 mm and metal width changed from 0.2 to 0.1 mm, in the same frequency in the range of 10-45 GHz. Figures (7-9) explain the real and imaginary parts of S11 and S21 parameters for all designs, respectively. The parts of real and imaginary of ε of the composite medium after the minified the dimensions of the designs has been calculated, and the results showed that the negative values of ε are about 5.7 to 21 GHz for sq-tr design, about 10 to 45 GHz for c-tr design, and about 10 to 13.955 GHz and 24.07 to 33.45 GHz as shown in figures (13-15). Then, the effective resonance frequency after the minified the dimensions of the designs has been calculated, and the results showed that the resonance frequency increases as shown in table (2).

The effect of the metal type of SRRs and rod was studied (PEC, aluminum, copper, gold and silver) and it was observed that there is no effect on the values of S-parameters.

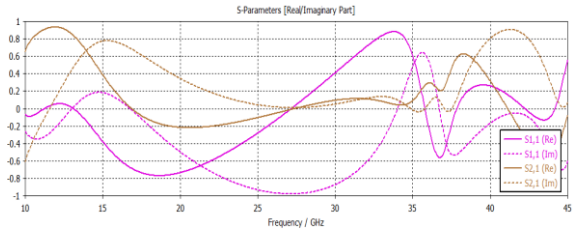

Fig. (5) Real and imaginary elements of the S11 and S21 SRR design parameters approximately 10-45 GHz for sq-tr design

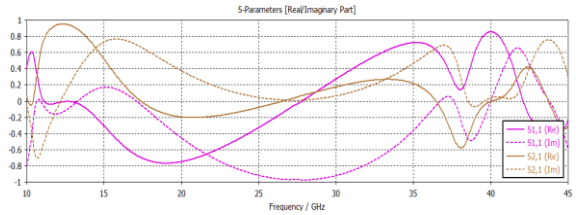

Fig. (6) Elements of the S11 and S21 real and imaginary sections of the c-tr SRR design parameters at 10-45 GHz

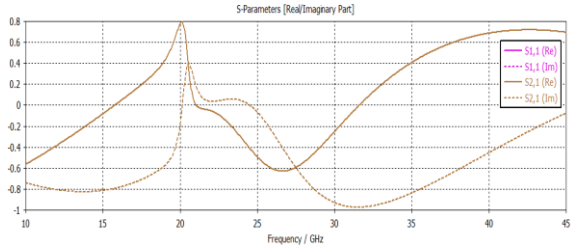

Fig. (7) The real and imaginary parts of S11 and S21 for the tr-tr design SRR at 10-45 GHz after change

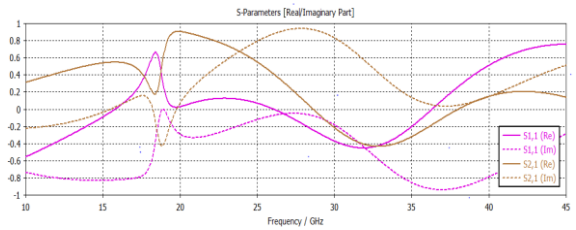

Fig. (8) The real and imaginary parts of S11 and S21 for the sq-tr design SRR at 10-45 GHz after change

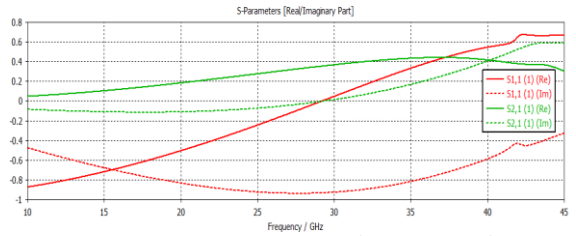

Fig. (9) The real and imaginary parts of S11 and S21 for the c-tr design SRR at 10-45 GHz after change

3. Results and Discussions

After the proper designs are completed, a simulation for frequency band 10-45 GHz was run, we sought to observe what effects varying the distances between d of the two rings for the three SRRs would have on the transmission through the element and substrate. While holding all other parameters constant (s, g, wt), then it concluded that the effective range of

frequencies that contains the peaks and dips under interest is between 17.525 to 21.165 GHz as in Fig. (4) for the tr-tr design, between 16.008 to 19.66 GHz as in Fig. (5) for the sq-tr design, and between 16.008 to 19.66 GHz as in Fig. (6) for the c-tr design. The results also showed that the largest value of resonant frequency is for the tr-tr design and then sq-tr and c-tr designs, as shown in table (1). Changing the d causes the resonance of the element to shift. This is due to the fact that the distance introduces a capacitance to the system that varies inversely with width of the gap, from a parallel plate system. The cause of this case that is when the distance between the two rings increased, the mutual capacitance between the two rings decrease, and the capacitance is [10]:

$$C = \varepsilon k \frac{A}{d} \quad (1)$$

where C is the capacitance of the element, ε is the permittivity of the medium in the area between the two rings, k is the dielectric strength of the medium, A is the area of the plates and d is distance between the two rings

Then the total capacitance will decrease [16]. In addition to that, the mutual inductance L decrease. So, the decrease in the total capacitance and inductance leads to an increase in effective resonance frequency, as in Eq. (2) [18]:

$$f = \frac{1}{2\pi\sqrt{L\varepsilon k\frac{A}{d}}} = \frac{1}{2\pi}\sqrt{\frac{A}{L\varepsilon k d}} \quad (2)$$

Then, the refractive index n_{eff} can be obtained by [5]:

$$n_{eff} = \frac{2}{jk_0 d}\sqrt{\frac{(S_{21}-1)^2 - S_{11}^2}{(S_{21}+1)^2 - S_{11}^2}} \quad (3)$$

where $k_0 = \frac{2\pi f}{c}$ is the wavenumber of vacuum, c refers to velocity of light [5]

Then, the values of real of ε_{eff} of all designs as shown in Fig. (10) have been retrieved from S-parameters utilizing post-processing of CST. For tr-tr design, the negative values of the real of ε_{eff} are about 10 to 20.115 GHz. Also, for c-tr design, the negative values of the real of ε_{eff} are about 10 to 12.485 GHz and 20.08 to 34.64 GHz, while for sq-tr design, the negative values of the real of ε_{eff} in about 10 to 12.1 GHz and 19.765 to 33.73 GHz, Furthermore, the negative values of μ_{eff} have been determined employing the same methodology as shown in Fig. (11). Figure (12) showed the increase of refractive index n_{eff} due to decreasing the total capacitance and inductance, where increase the distance between the two rings produces the increase increasing in effective resonance frequency. The n_{eff} has negative values around this range. This frequency range corresponds to the band of LH transmission. By looking to Fig. (12), it can be concluded that the largest value of effective refractive index is for the design tr-tr and then c-tr and sq-tr, and n_{eff} exhibits a negative values as shown in table (1).

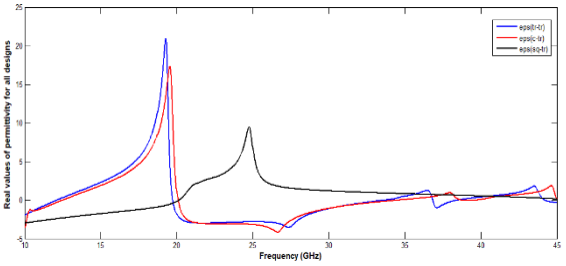

Fig. (10) Real parts of electric permittivity ε_{eff} for all designs

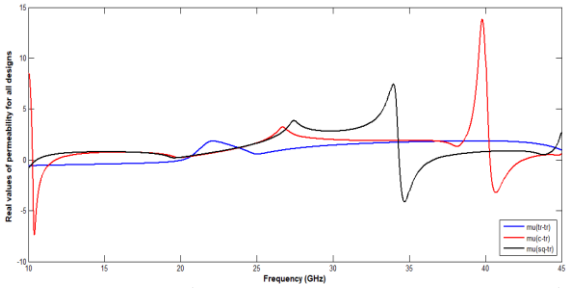

Fig. (11) Real parts of magnetic permeability μ_{eff} parameters for all designs

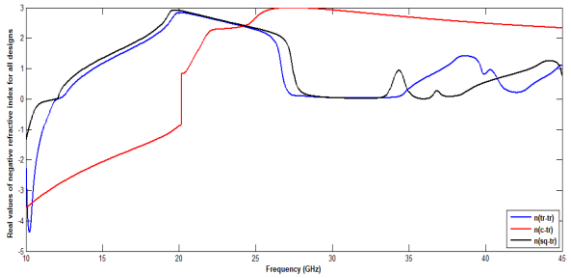

Fig. (12) Real parts of refractive index n_{eff} for all designs

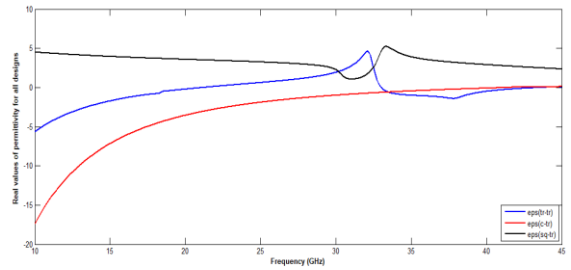

Fig. (13) Real parts of electric permittivity ε_{eff} for all designs after change

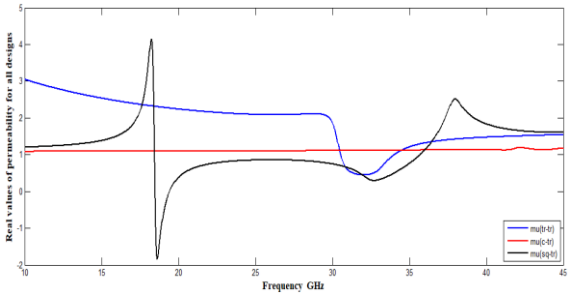

Fig. (14) Real parts of magnetic permeability μ_{eff} parameters for all designs after change

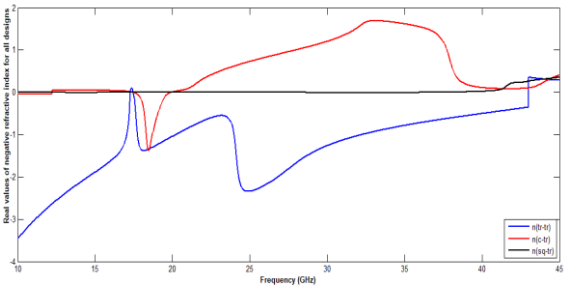

Fig. (15) Real parts of refractive index n_{eff} for all designs after change

The use of triangular resonators in RADAR and satellite communications indeed presents a unique challenge when it comes to determining the frequency of resonance, especially with the variety of triangular shapes. For more complex geometries, such as irregular triangles, the calculation of the frequency of resonance can be more demanding due to the need to account for factors like boundary conditions and the distribution of electromagnetic fields. All three geometrical designs of the SRRs printed on similar dielectric substrates, were studied in same physical dimensions. These resonators' resonance behaviour was verified by measuring and modeling transmission via a single SRR unit cell. The comparison of their frequency of resonance, which determines the region of negative μ. Finally, the S-parameters together with the μ_{eff} and ε_{eff} data were used to calculate the effective refractive index neff of LH media for the different designs. The values of negative μ, negative ε, and negative refractive index using a numerical technique of CST studio has been approved of different metamaterial design. The composite medium of conducting, non-magnetic elements can form a frequency band of LH, where the ε_{eff} and the μ_{eff} are simultaneously negative. The S-parameters are affected by changing the dimensions of SRRs with changing the dimensions. Decreasing these dimensions leading to an increase in S11 and S21.

4. Conclusions

The frequency of resonant is affected by changing the dimensions of SRRs with changing with changing the dimensions. Increasing these parameters leading to an increase in frequency of resonant. The effective negative refractive index is affected by changing the dimensions of SRRs with changing with changing the dimensions. Decreasing these parameters leading to decrease in effective negative refractive index. There is no effect of the material type of the SRRs and rod metal on the results of S-parameters and the frequency of resonance. The SRRs shape is changed to have three designs which are triangle-triangle, circle-triangle and square-triangle. It found that the frequency of resonant is largest for triangle-triangle, then circle-triangle and finally square-triangle. The results reveal that frequency of resonant of metamaterials can be controlled by the design of resonators and hence in achieving the bulk metamaterials with negative permeability.

References

[1] A. Sarkar and G.C. Maity, "Momentum-space properties for ground and Rydberg states of lithium atom", *Brazillian J. Phys.*, 52 (2002) 92.

[2] T. Ramachandran, M. R. Faruque and K. S. Al mugren, "Symmetric left- handed split ring resonator metamaterial design for terahertz frequency applications", 13(1) (2007).

[3] L.J. Roglá, J. Carbonell and V.E. Boria, "Study of equivalent circuits for open- ring and split- ring resonators in coplanar waveguide technology", *IET Microwaves Antennas Propag.*, 1(1) (2007) 170-176.

[4] S. Zahertar, A. D. Yalcinkaya and H. Torun, "Under different excitations at microwave frequencies", *AIP Advances*, 5(11), (2005).

[5] C.G. Parazzoli et al., "Experimental determination and numerical simulation of the properties of negative index of refraction materials", *Opt. Exp.*, 11(7) (2003) 688-695.

[6] D.R. Smith et al., "Composite Medium with Simultaneously Negative Permeability and Permittivity", *Phys. Rev. Lett.*, 84 (2000) 18.

[7] F.E. Zerrad et al., "Multilayered metamaterials array antenna based on artificial magnetic conductor's structure for the application diagnostic breast cancer detection with microwave imaging", Med. Eng. Phys., 99 (2022) 103737.

[8] F.H. Bautista, C.A. Vargas and J.M.A. Arcos, "Negative refractive index in split ring resonators", Materials, 59(1) (2013), 141-146.

[9] G. Parisi, "Propagation of electromagnetic waves in "Fishnet" metamaterials", PhD thesis, University of Padua (Italy, 2012).

[10] S. Zahertar, A. D. Yalcinkaya and H. Torun, "Rectangular split-ring resonators with single-split and two-splits under different excitations at microwave frequencies", *AIP Advances*, 5(11), (2015).

[11] I.A. Buriak et al., "Metamaterials: Theory, Classification and Application Strategies (Review)", *J. Nano Electron. Phys.*, 8(4(2)) (2016) 04088-1-11.

[12] I.N. Idrus et al., "An Oval-Square Shaped Split Ring Resonator Based Left-Handed Metamaterial for Satellite Communications and Radar Applications", *Micromachines*, 13 (2022) 578.

[13] K. Aydın, "Characterization and application of negative- index metamaterials", PhD thesis, Bilkent University (Turkey, 2008).

[14] K. Aydin et al., "Investigation of magnetic resonances for different split-ring resonator parameters and designs", *New J. Phys.*, 7 (2005) 168.

[15] K. Aydin and E. Özbay, "Experimental and numerical analyses of the resonances of split ring resonators", *phys. stat. sol. (b)*, 244(4) (2007) 1197-1201.

[16] M.M. Khan et al., " Design and analysis of a 5G wideband antenna for wireless body-centric network", *Wireless Commun. Mobile Comput.*, 2022 (2022) 1558791.

[17] K. Doppler et al., "Future indoor network with a sixth sense: requirements, challenges and enabling

technologies", *Pervasive Mobile Comput.*, 83 (2022) 101571.

[18] M. Berka, A. Bendaoudi and Z. Mahdjoub, "Triangular Split Ring Resonators for X-Band Applications and Operations", *J. Nano Electron. Phys.*, 14(1) (2022) 01007-1-5.

[19] M.K. Al-Nuaimi and W.G. Whittow, "Compact microstrip band stop filter using SRR and CSSR: Design, simulation and results", *IEEE Proceed. 4th Euro. Conf. on Antennas and Propag.*, 12-16 April 2010, pp. 1-5.

[21] M.L. Hakim et al., "Quad-Band Polarization-Insensitive Square Split-Ring Resonator (SSRR) with an Inner Jerusalem Cross Metamaterial Absorber for Ku- and K-Band Sensing Applications", *Sensors*, 22 (2022) 4489.

[22] N. Ullah et al., "A compact complementary split ring resonator (CSRR) based perfect metamaterial absorber for energy harvesting applications", *Eng. Sci. Technol.*, 45 (2023) 101473.

[23] A. Nyirady, "Kacific reveals plans for second satellite, Via Satellite", October, 30th, 2020, http://www.satellitetoday.com/launch/2020/10/30/kacific-reveals-plans-for-second-satellite/.

[24] R. Marcelli et al., "Triangular Sierpinski Microwave Band-Stop Resonators for K-Band Filtering", *Sensors*, 23 (2023) 8125.

[25] S.L. Madsen and J.S. Bobowski, "The Complex Permeability of Split-Ring Resonator Arrays Measured at Microwave Frequencies", *IEEE Trans. Microwave Theory Tech.*, 68(8) (2020) 3547-3557.

[26] S. Lalithakumari et al., "Analysis of wave propagation in hybrid metamaterial structure for terahertz applications", *Braz. J. Phys.*, 53 (2023) 140.

[27] S.P. Antipov et al., "Left- handed metmaterials stuies and their application", *IEEE Proceed. 2005 Particle Accelerator Conf.*, Knoxville, Tennessee (USA, 2005).

[28] S. Li et al., "A Novel Tunable Triple-Band Left-Handed Metamaterial", *Int. J. Antennas Propag.*, 2017 (2019) 7583736.

[29] A.K. Singh, M.P. Abegaonkar and S.K. Koul, "Metamaterials for antenna applications", 1st ed., CRC Press (2021).

[30] S.S. Bukhari, J. Vardaxoglou and W. Whittow, "A Metasurfaces Review: Definitions and Applications", *Appl. Sci.*, 9 (2019) 2727.

[31] T.K. Esogu and M.Ö. Esogu, "Electrically Small Split Ring Resonator Antennas Epsilon and Gain Analysis", Antenna Theory: Dr. Öğr. Hayrettin Odabaşi, 1 (2020) 1.

[32] T. Ramachandran, M.R.I. Faruque and M.T. Islam, "Symmetric square shaped metamaterial structure with quintuple resonance frequencies for S, C, X and Ku band applications", *Sci. Rep.*, 11 (2021) 4270.

[33] T.A.K. Al-musawi, "Investigation the Optical Properties of Some Negative Refractive Index Metamaterials", Ph.D. thesis, University of Kufa (Iraq, 2022).

[34] T.A.K. Al-musawi, S.A. Mahdi and S.Y.H. AL-Asadi, "Characteristics of circle- square SRR left handed materials", *J. Optoelectron. Laser*, 41 (2022) 7.

[35] V. Jagadeesan et al., "Design and development of a new metamaterial sensor-based Minkowski fractal antenna for medical imaging", *Appl. Phys. A*, 129 (2023) 391.

[36] V. P. Yadav et al., "Use of Metamaterials in Antenna Design: A Review", *JETIR*, 7 (2020) 12.

[37] M.R. Vidhyalakshmi, B. Rekha and P.H. Rao, "Stopband Characteristics of Complementary Triangular Split Ring Resonator Loaded Microstrip Line", *IEEE Appl. Electromag. Conf. (AEMC)*, India (2011).

[38] W. J. Padilla et al., "Left- handed metamaterials", *NATO-ASI, Photonic Crystals and Light Localization* (2000).

[39] N. Yu et al., "Light propagation with phase discontinuities: generalized laws of reflection and refraction", *Science*, 334(6054) (2011) 333-337.

[40] Z. Jakšić, N. Dalarsson and M. Maksimovi, "Negative Refractive Index Metamaterials: Principles and Applications", *Microwave Rev.*, (2006) 36- 49.

Table (1) Effective resonance frequency for different designs

No.	Type of SRR	the designs dimensions			Effective resonance frequency		Effective refractive indes
		g (mm)	wt (mm)	s (mm)	f_{S11} (GHz)	f_{S12} (GHz)	n_{eff}
1	triangle- triangle (tr- tr) SRR	0.2	0.2	1.14	17	17	-4.367
2	square- triangle (c- tr) SRR	0.2	0.2	1.14	12.24	12.24	-3.574
3	circle- triangle (sq- tr) SRR	0.2	0.2	1.14	10.315	10.28	-1.315

Table (2) Effective resonance frequency for different designs after change

No.	Type of SRR	the designs dimensions			Effective resonance frequency		Effective refractive index
		g (mm)	wt (mm)	s (mm)	f_{S11} (GHz)	f_{S12} (GHz)	n_{eff}
1	triangle- triangle (tr- tr) SRR	0.1	0.1	1.14	33.36	33.36	-3.452
2	square- triangle (c- tr) SRR	0.1	0.1	1.14	42.305	36.915	-1.378
3	circle- triangle (sq- tr) SRR	0.1	0.1	1.14	18.4	18.365	-0.0086

